ACADEMIC PRESS

Available online at www.sciencedirect.com
SCIENCE DIRECT®

NeuroImage

NeuroImage 19 (2003) 1049–1060

www.elsevier.com/locate/ynimg

A novel method for noninvasive detection of neuromodulatory changes in specific neurotransmitter systems

Nathaniel M. Alpert,* Rajendra D. Badgaiyan, Elijahu Livni, and Alan J. Fischman

Division of Nuclear Medicine, Massachusetts General Hospital, Boston, MA 02114, USA

Received 2 December 2002; revised 13 February 2003; accepted 18 March 2003

Abstract

Over the last decade, it has become possible to study theories of cognition using positron emission tomography (PET) and functional magnetic resonance imaging (fMRI). These methods yield statistical parametric maps of changes in cerebral blood flow (CBF) elicited by cognitive tasks. A limitation of these studies is that they provide no information about the underlying neurochemistry. However, it is possible to extend the concept of activation studies to include measurements targeting neurotransmitters and specific receptor populations. Cognitive activation increases neuronal firing rate, increasing the endogenous neurotransmitter level. The increased neurotransmitter level can be used to alter the kinetics of specifically bound radioligands. We describe a new approach to the design and analysis of neuromodulation experiments. This approach uses PET, a single-scan session design, and a linear extension of the simplified reference region model (LSSRM) that accounts for changes in ligand binding induced by cognitive tasks or drug challenge. In the LSSRM, an "activation" parameter is included that represents the presence or absence of change in apparent dissociation rate. Activation of the neurotransmitter is detected statistically when the activation parameter is shown to violate the null hypothesis. Simulation was used to explore the properties of the LSSRM with regard to model identifiability, effect of statistical noise, and confounding effects of CBF-related changes. Simulation predicted that it is possible to detect and map neuromodulatory changes in single-subject designs. A human study was conducted to confirm the predictions of simulation using ^{11}C-raclopride and a motor planning task. Parametric images of transport, binding potential, areas of significant dopamine release, and statistical parameters were computed. Examination of the kinetics of activation demonstrated that maximum dopamine release occurred immediately following task initiation and then decreased with a half-time of about 3 min. This method can be extended to explore neurotransmitter involvement in other behavioral and cognitive domains.

Introduction

In recent years positron emission tomography (PET) and functional magnetic resonance imaging (fMRI) techniques have been used to detect changes in cerebral blood flow (CBF) elicited by cognitive or behavioral tasks. These "activation" studies have successfully identified a number of cortical and subcortical areas that process a variety of cognitive activities. However, these experiments are limited by their inability to identify cellular mechanisms associated with cognitive changes. Since the CBF-related changes are nonspecific, these studies do not provide information about the nature of the underlying neurochemistry and neurotransmitter systems involved in performing specific cognitive tasks. Because of these limitations, activation studies are not likely to explain neurophysiological mechanisms of cognition. One of the challenges for neuroimaging experiments is to advance the methodology to the point where one can not only identify the regions of brain that are activated by a stimulus, but also determine the chemical systems that mediate these responses (Coull, 1998; Granon et al., 2000; Kahkonen et al., 2001; Lawrence et al., 1998).

Experiments conducted on human volunteers and laboratory animals have provided reliable data suggesting that neurotransmitters and neuromodulators significantly influence a variety of cognitive functions (Jentsch et al., 2000; Kulisevsky, 2000; Oak et al., 2000; Robbins, 2000; Robbins et al., 1997). It has been shown that activation or inhibition of neurotransmitter systems causes significant alteration in performance of human volunteers and laboratory animals on a variety of tasks of spatial attention (Jackson et al., 1994; Perry et al., 1999; Witte and Marrocco, 1997; Robbins, 2000), and working memory (Granon et al., 2000; Greenwald and Davis, 1983; Jaber et al., 1996; Kimberg et al.,

* Corresponding author. Fax: +1-617-726-6165.
E-mail address: alpert@pet.mgh.harvard.edu (N.M. Alpert).

1053-8119/03/$ – see front matter © 2003 Elsevier Science (USA). All rights reserved.
doi:10.1016/S1053-8119(03)00186-1

2001). There is, however, no direct evidence that associates a specific neurotransmitter system with a cognitive function.

In 1995 Fisher et al. and Morris et al. suggested that it might be possible to use PET and specifically bound radioligands to detect changes in the binding kinetics of reversibly bound radioligands. The prediction was based on the idea that neurons involved in a cognitive task increase their firing rate, causing an increase in the synaptic level of endogenous neurotransmitter. This mechanism can be used to perturb the kinetics of specifically bound receptor ligands, making it possible to detect the effect with PET. Koepp et al. (1998) performed the first study testing the feasibility of the idea; but their experiment involved a complex task (a video game) and required two scan sessions and a cohort of subjects to detect an effect. A ground-breaking study by Friston et al. (1997) proposed and demonstrated a method for assessing time-dependent changes in ligand displacement by using a single-scan design and a pharmacological challenge. Recently, Pappata et al. (2002) have applied and extended Friston's method to study a gambling/reward task. In this study, we present a novel methodology designed to increase the sensitivity of single-scan session designs so that activation might be detected in individual subjects. This report presents the theory, discusses its implementation, evaluates elements of the theory by simulation, and demonstrates feasibility in a human experiment.

Theory

We derive a kinetic theory capable of describing non-steady-state (i.e., time dependent) fluctuations of receptor parameters. This theory rests on the reference region models (Lammertsma et al., 1996) and the simplified reference region model (SRRM) of Lammertsma and Hume (1996) and Gunn et al. (1997). Our theory extends the SRRM in two ways: first, it allows the parameters to be time dependent and second, all parameters enter linearly. To review briefly, the SRRM follows from the following basic equations:

$$\frac{dC(t)}{dt} = K_{1a}C_p(t) - k_{2a}C(t) \tag{1}$$

$$\frac{dC_r(t)}{dt} = K_{1r}C_p(t) - k_{2r}C_r(t) \tag{2}$$

$C_p(t)$ denotes the plasma concentration of radioligand at time t. C and C_r are instantaneous quantities denoting radioactivity concentration in a binding and reference region respectively. The reference region is assumed to be devoid of specific binding. The subscript r refers to the reference region parameters and the subscript a refers to an "apparent" volume containing both free and nonspecifically bound tracer as well as specifically bound tracer. This apparent volume is assumed to be adequately described by a single compartment model, with the bound and free tracer in instantaneous equilibrium. In the limit of instantaneous equilibrium, the SRRM parameters are related to the standard receptor model with two compartments and four parameters, K_1, k_2, k_3, and k_4. By assuming that the volume of distribution of the nonspecifically bound tracer is the same in the reference and the binding region, one can derive a series of convenient equations. By substitution for C_r, the binding equation can be rewritten as

$$\frac{dC(t)}{dt} = \frac{K_{1a}}{K_{1r}}\left[\frac{dC_r(t)}{dt} + k_{2r} \cdot C_r(t)\right] - k_{2a} \cdot C(t) \tag{3}$$

and directly integrated to yield

$$C(t) = RC_r(t) + k_2\int_0^t C_r(u)du - k2a\int_0^t C(u)du \tag{4}$$

where:

$$R = \frac{K_{1a}}{K_{1r}} = \frac{k_2}{k_{2r}}$$

$$k_{2a} = \frac{k_2}{1 + BP}$$

$$BP = \frac{k_3}{k_4}$$

Including the effect of activation

In this theory we consider activation to be any cognitive effect or drug challenge that can render any, or all, of the model parameters to be time dependent, i.e., the non- steady-state situation. For this approach to be useful we have to "know" or hypothesize the time dependence of the parameters. In addition to changes in the endogenous neurotransmitter level, changes in blood flow may cause time-dependent changes in the model parameters (Dagher et al., 1997; Pappata et al., 2002). The non-steady-state equation is obtained by integrating Eq. (3) assuming that the parameters are time dependent.

$$C(t) = \int_0^t R(u) \cdot \frac{dC_r}{du}\,du + \int_0^t k_2(u) \cdot C_r(u)du - \int_0^t k_{2a}(u) \cdot C(u)du \tag{5}$$

We propose a basic activation model that includes a control state with parameters R, k_2, and k_{2a}. The activation state is parameterized as $R + \alpha\, h(t)$, $k_2 + \beta\, h\,(t)$, and $k_{2a} + \gamma\, h(t)$, where we assume a common time dependence for the activated state described by $h(t)$. The basic equation is:

$$C(t) = RC_r(t) + k_2\int_0^t C_r(u)du - k_{2a}\int_0^t \cdot C(u)du + \alpha\int_0^t \frac{dC_r}{du}h(u)du + \beta\int_0^t C_r(u)h(u)du - \gamma\int_0^t C(u)h(u)du \tag{6}$$

Because there is a paucity of relevant experimental data, it is not possible to specify $h(t)$ with great certainty. Based on the available data (see Fisher et al., 1995), we can assume that changes in endogenous neurotransmitter levels occur on a time scale that is very fast compared to PET imaging times. The available data also support the assumptions that the major effects of activation occur immediately after the onset of the task and that the effects diminish over time. More discussion of this point is presented later. For the purpose of this study we consider an exponential form for $h(t)$ (Endres and Carson, 1998), with activation commencing at time T.

$$h(t) = \begin{bmatrix} 0, & t < T \\ e^{-\tau(t-T)}, & t \geq T \end{bmatrix} \tag{7}$$

where τ controls the rate at which activation effects die away. The model equation

$$C(t) = \begin{bmatrix} RC_r(t) + k_2\int_0^t C_r(u)du - k_{2a}\int_0^t C(u)du & 0 < t < T \\ RC_r(t) + k_2\int_0^t C_r(u)du - k_{2a}\int_0^t C(u)du + \ldots & \\ \alpha\left[(C_r(t)e^{-\tau(t-T)} - C_r(T)) + \tau\int_T^t C_r(u)e^{-\tau(u-T)}du\right] + \ldots & \\ \beta\int_T^t e^{-\tau(u-T)}C_r(u)du - \gamma\int_T^t e^{-\tau(u-T)}C(u)du & t > T \end{bmatrix} \tag{8}$$

predicts the instantaneous concentration curve.

To derive an operational equation for this theory, we take note of the fact that the concentrations in Eq. (8) are instantaneous quantities. Denote the measurable quantities as *pet* and *ref*. *pet* is the concentration value measured by the PET scanner in a binding region and *ref* is the concentration measured in a region devoid of specific binding. In terms of the instantaneous quantities the ith measurement is

$$pet_i = \frac{1}{\Delta_i}\int_{t_i}^{t_i+\Delta_i} C(u)du \tag{9}$$

$$ref_i = \frac{1}{\Delta_i}\int_{t_i}^{t_i+\Delta_i} C_r(u)du \tag{10}$$

where Δ_i represents the duration of the ith frame and t_i is the start time of the ith frame. Integrating Eq. (8), we can closely approximate the integrals as sums, yielding an operational equation suitable for numeric computation,

$$pet_i \approx \begin{bmatrix} 1 \leq i < j_s & \\ R \cdot ref_i + k_2\left(\sum_{j=1}^{j=i}\Delta_j ref_j - \frac{1}{2}\Delta_i \cdot ref_i\right) - k_{2a}\left(\sum_{j=1}^{j=i}\Delta_j pet_j - \frac{1}{2}\Delta_i \cdot pet_i\right) & \\ i \geq j_s & \\ R \cdot ref_i + k_2\left(\sum_{j=1}^{j=i}\Delta_j ref_j - \frac{1}{2}\Delta_i \cdot ref_i\right) - k_{2a}\left(\sum_{j=1}^{j=i}\Delta_j pet_j - \frac{1}{2}\Delta_i \cdot pet_i\right) + \ldots & \\ \alpha \cdot (ref_i \cdot e^{-\tau(t_i+\Delta_i/2+T)} - ref_{j_s}) + \ldots & \\ + \tau \cdot \left(\sum_{j=j_s}^{j=i} ref_j \cdot e^{-\tau(t_j+\Delta_j/2+T)} - \frac{1}{2}\Delta_i ref_i e^{-\tau(t_i+\Delta_i/2+T)}\right)\ldots & \\ - \gamma \cdot \left(\sum_{j=j_s}^{j=i}\Delta_j \cdot pet_j \cdot e^{-\tau}(t_j + \Delta_j/2 - T) - \frac{1}{2}\Delta_i \cdot pet_i \cdot e^{-\tau(t_i+\Delta_i/2-T)}\right) & \end{bmatrix} \tag{11}$$

where j_s is the frame in which the activation task begins.

Table 1
Simulation parameters

Reference region		Binding region						LSSRM				
K_{1R}	k_{2R}	K_1	k_2	k_3	k_4	R	BP	R	k_2	k_{2a}	BP	Notes
0.092	0.45	0.092	0.45	0.062	0.014	1	4.54	0.83	0.29	0.052	4.57	[a]
0.18	0.326	0.18	0.37	0.38	0.11	1	3.45	0.85	0.20	0.044	3.50	[b]

[a,b] Adapted from [a]Pappata et al. (2002) and [b]Farde et al. (1989), Subject C. The parameters listed in the Binding region section of the table were those indicated in notes [(a)] and [(b)] and they were used to simulate positron emission tomographic (PET) curves with the standard two compartment PET receptor model. The parameters listed under LSSRM were those estimated with the linear simplified reference region model.

Parameter estimation and hypothesis testing

To simplify the exposition, assume that τ is known; we will describe how we estimated τ in the materials and methods section of this report. With this assumption, the model equations are linear in the parameters. We will refer to this as the linear simplified reference region model (LSSRM). Linear least squares provides estimates of the model parameters and their covariance matrix. In statistical parlance, the effects of interest are R, k_2, k_{2a}, α, β, and γ, with γ being the parameter of greatest interest. An important point in this study is that while the LSSRM provides quantitative estimates of the parameters, our interest will often be satisfied if we can reject the null hypothesis $\gamma \leq 0$. Simple hypotheses are tested by using the estimated covariance matrix to compute t statistics for the parameters of interest (Searle, 1971; Friston et al., 1995; 1997). The t statistic has $n - p + 1$ degrees of freedom where n is the number of frames and p the number of model parameters. For region of interest (ROI) analysis, the percentage points of the t distribution can be used to test for significance. For parametric imaging, the use of random field theory and the concepts of SPM analysis (Friston et al., 1995, 1997) is required to set appropriate significance thresholds when there are no apriori localizing hypotheses. In principle, hypothesis testing can detect significant changes in α and β, protecting against CBF-related confounds with changes in γ; but whether this can be achieved in practice depends on the identifiability of the model parameters. We will return to this point in the discussion.

Materials and methods

To evaluate the theory we performed simulation studies and experiments with human subjects. The simulations examine basic questions about model, parameter identifiability in the face of random noise, and the confounding effects of changes in blood flow. The human studies attempt to demonstrate the feasibility of detecting changes in receptor binding due to a motor planning task. For this study we use a single human study as an example to show proof of principle; the results of the human studies have been reported elsewhere (Badgaiyan et al., 2003).

Simulation studies

All simulations were programmed in the MATLAB computing environment (Release 13, The Mathworks, Natick, MA). Differential equations were solved using ode23s, a solver designed for so-called stiff equations. To mimic experimental protocols, we simulated an acquisition with 59 frames (10 at 30 s, 45 at 1 min, and 4 at 5 min). Fitting parameters and their covariance matrix were determined analytically, using weighted linear least squares.

The first set of simulations addressed the issue of biased estimation by comparing the LSSRM with the standard four-parameter, two-compartment model of receptor binding, as applied to ^{11}C-raclopride. The endpoint of the simulation was to determine whether the LSSRM could fit data generated with the standard model and whether the LSSRM parameters matched the values used in the standard model. The instantaneous values for reference and binding region concentrations were determined by solving the corresponding differential equations with parameters appropriate to raclopride binding (see Table 1), using a measured input function. The expected values for the PET curves (i.e., simulated) were determined by integrating the instantaneous concentration values to compute the average concentrations for the simulated scan protocol. The simulated reference region curve was used as the input function with Eq. (11) and linear least squares estimation to "fit" the simulated binding curve (α, β, and γ were set to 0). The same calculation was also performed with the original method of Gunn et al. (1997), which solves the nonlinear SRRM equations by a combination of linear least squares and table lookup.

The second set of simulations, again with noise-free data, studied a range of possible effects that may accompany cognitive activation or pharmacological challenge. These include the effects of increased ligand displacement and increased blood flow. We considered possibilities such as proportional increase in K_1 and k_2, so that the distribution volume remained constant, and separate changes in k_2 and k_1. The differential equations were modified to allow for time-dependent parameters. All of these simulations assumed a time-dependent parameter(s) of the form

$$p(t) = \begin{bmatrix} p_o & t \leq T \\ (p_o + \delta p)e^{-\tau(t-T)} & t > T \end{bmatrix} \quad (12)$$

Simulations were performed for perturbations beginning at $T = 38$ min after injection. Tests were performed to

determine the degree of bias in the parameters, the goodness of fit, and model identifiability.

The third set of simulations examined the feasibility of detecting ligand displacement in individual subjects at the voxel level. In essence, these simulations examined the effect of statistical noise on detection of effects. We simulated PET curves with the LSSRM and the parameters R, k_2, and k_{2a} shown in Table 1 for Subject C in Farde et al. (1989). The effect of increased dopamine level was set as described above. Simulation of noisy data was computed by adding Gaussian random noise with variance proportional to $C_m \cdot e^{\lambda t}/dt$, where C_m was the peak value of the noise-free simulation and λ denotes the decay constant for ^{11}C. The proportionality constant was adjusted to yield results similar to that observed in human studies with racolpride at a spatial resolution of ~10 mm. To gauge the level of type II error that might affect this type of analysis, we analyzed another ensemble of 10,000 simulations having the same noise level added to a simulation with $\gamma = 0$.

Human studies

A set of pilot studies studies were performed in 5 young healthy human volunteers, under the supervision of the Committee on Human Research at the Massachusetts General Hospital. The general nature of the experiments was explained and subjects gave written informed consent. The object of these initial studies was to test the predictions of simulations suggesting the possibility of detecting ligand displacement in individual subjects during a well-defined motor planning task. Because this study is methodological in nature and because the results of the human study will be of interest to a wider community, we present the results of one study in this report.

The test subject reported here received a bolus injection (1 min duration) of ~14 mCi of ^{11}C-raclopride, with specific activity 900 mCi/μmol, in the left antecubittal vein. The subject was imaged in the supine position with head restrained by a custom-molded thermoplastic mask, using an ECAT EXACT HR$^+$ PET scanner operating in the three-dimensional mode. The ECAT HR$^+$ records 63 slices simultaneously, with an intrinsic resolution of about 4-mm FWHM in all spatial dimensions (Adam et al., 1997). The acquisition protocol recorded frames over a 90-min period. Images were reconstructed as 128 × 128 × 63 element volumes using an OSEM algorithm, with corrections for photon attenuation, random coincidences, scatter, and dead time. To minimize the residual effects of head movements, image registration was performed to align each frame to a common orientation (Alpert et al., 1996). To effect the image registration, we used the following multistep procedure: First, all frames were smoothed with a 10-mm FWHM Gaussian filter. Second, all frames were aligned to the frame taken at 25 min. Next, the aligned frames were summed to form a new reference volume and all frames were aligned again to the sum image.

A task was designed to focus on motor planning. The core element of the task was the opposition of the thumb and fingers in response to visual cues presented on a computer monitor. The same visual cues, the presentation of a single random digit (1, 2, 3, or 4) once every 2 s, were visible to the subject throughout the experiment. During the control phase of the study, the subject was instructed to lie still without moving. In the study presented here finger opposition started 38 min after raclopride injection and continued for the duration of the experiment. The subject was instructed to oppose the right thumb and forefinger upon seeing the digit 1, their thumb and middle finger on seeing the digit 2, and so on. Compliance with all instructions was observed by closed-circuit television.

Image analysis was performed by using a combination of ROI analysis and parametric imaging. Visual examination of the image data was used to identify the cerebellum, a three-dimensional ROI was defined, and a time activity curve (TAC) was extracted to serve as the reference region TAC. All frames were smoothed with a 10-mm FWHM Gaussian filter. To reduce the computational load, a mask indicating the "important voxels" was determined by summing all frames and using a threshold 1.3 times the mean of all voxels. The LSSRM model with α and β fixed to zero was used to fit all voxels within the mask. Parametric images of the R, k_2, k_{2a}, $BP = k_2/k_{2a} - 1$, γ, the covariance matrix, and the t score for γ were computed. A presentation image of the t map for the γ parameter was determined by including only those voxels for which $k_2 - 1.5 \cdot k_{2a} > 0$. In the fusion of the t map and binding potential, the binding potential image was filtered with a 3 × 3 median filter to suppress high frequency noise.

The analysis proceeded as a two-step process. First, data were analyzed assuming $h(t)$ was a step function (*i.e.*, $\tau = 0$). Following that analysis the t map was examined for evidence of increased ligand displacement. Regions of increased displacement were further analyzed by ROI analysis. TACs were extracted and fit with a model that allowed τ to vary. Following estimation of τ, the parametric maps were recomputed.

Statistical analysis

The LSSRM model uses weighted linear least squares analysis for parameter estimation. The theory of least squares analysis also provides an estimate of the covariance matrix of the parameters [see Friston et al. (1997) for relevant details]. Accordingly, parameter values are presented with estimates of their standard error (SE). The hypothesis $\gamma \leq 0$ is tested by computing $t = \gamma/\mathrm{SE}(\gamma)$.

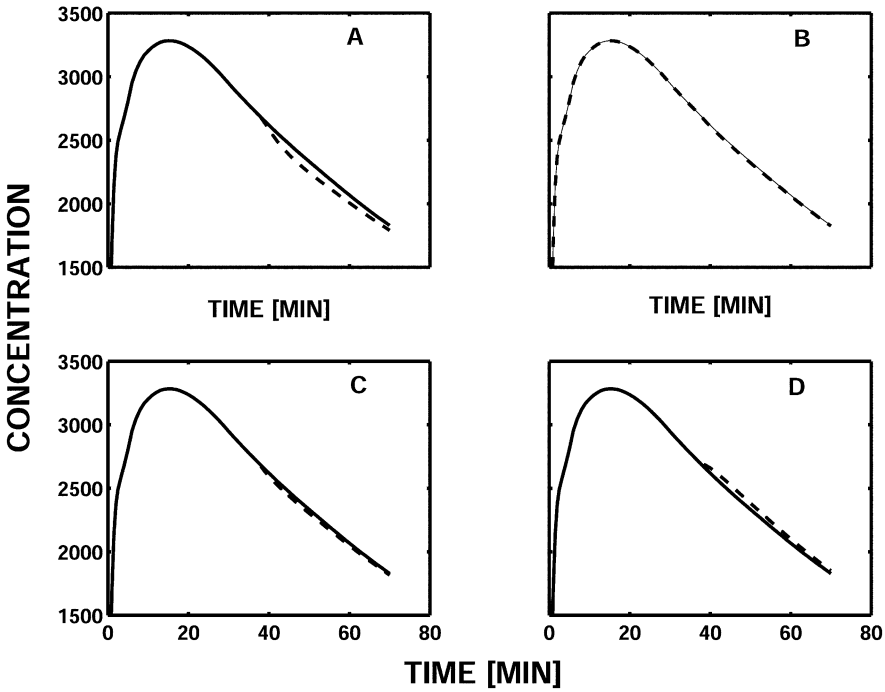

Fig. 1. Simulation of raclopride kinetics. In all cases the solid line is the control condition (see Table 1 for details) and all effects begin 38 min post injection with $\tau = 0.22$ 1/min. (A) 33% increase in endogenous dopamine. (B) 20% increase in both K_1 and k_2. (C) 20% increase in k_2 with K_1 unchanged. (D) 20% increase in K_1.

Results

Basic simulations

In all cases the LSSRM made excellent fits to the simulated noise-free data. With graphical display, only very small differences between data and fit could be seen. However, as seen in Table 1, the parameter values for the LSSRM were biased and, as expected from the structure of the model, the covariance matrix of the parameter estimates showed high correlation between k_2 and k_{2a}. Despite this bias, values of binding potential determined from $BP = k_2/k_{2a} - 1$ were close to the "true value." The same simulation performed with the original nonlinear method, described by Gunn et al. (1997), gave very similar results, with the small differences likely due to the difference in fitting method employed.

Simulation

Fig. 1 shows simulations that predict the kinetics of raclopride under the following four conditions: (1) displacement resulting from increased levels of endogenous dopamine; (2) perturbation resulting from increases in K_1 and k_2 (holding the distribution volume constant); (3) displacement resulting from increase of k_2; and (4) perturbation resulting from increase in K_1. These data illustrate the magnitude of the effects. Increasing transport and clearance 20% while holding the distribution volume constant has negligible effect; whereas, 20% increases in k_2 alone may be difficult to separate from displacement due to increasing levels of endogenous dopamine. Increasing K_1 results in an increased PET concentration. Fitting the LSSRM model to these data yielded good fits to the simulation curves and the differences between simulation and fit were difficult to visualize with graphical display. All cases could be fit with $\alpha = 0$ and $\beta = 0$; in the case of increased K_1, the estimates of γ were negative. When two or more of the "activation" parameters were included, the estimates were unreliable. Examination of the covariance matrix of the parameter estimates showed very high correlation among two or more activation parameters. We will discuss this point more fully later.

Simulation 3, effect of statistical noise

Fig. 2 shows an example of the LSSRM fit to noisy data. The parameters of this fit were close to the input values, $R = 0.854 \pm 0.020$, $k_2 = 0.195 \pm 0.004$, $k_{2a} = 0.043 \pm 0.001$, and $\gamma = 0.020 \pm 0.004$. For an ensemble of 10,000 simulations with $\gamma \neq 0$, the mean t score for estimation of $\gamma \neq 0$ was 3.7. Examination of the distribution of t scores obtained for the ensemble showed that t was greater than 3 in 93% of the simulations. When the same simulation was run with $\gamma = 0$, we found the mean t score for estimation of $\gamma \neq 0$ was -0.07, with 7% of t scores greater than 2 and 0.7% greater than 3.

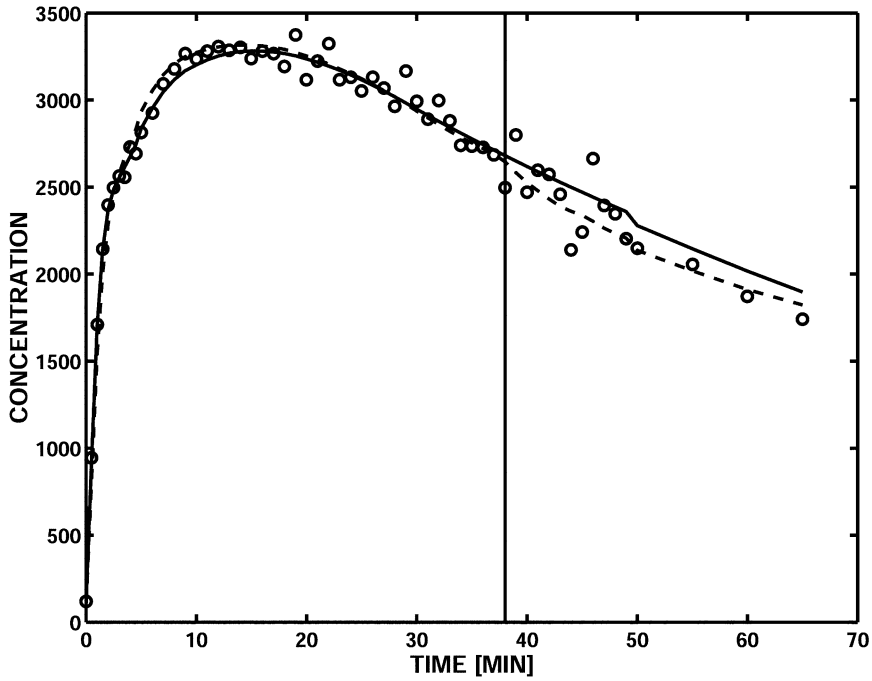

Fig. 2. Effect of noise on raclopride kinetics. The solid line is the control condition (see Table 1 for details) and all effects begin 38 min post injection with $\tau = 0.22$ 1/min. Simulation of 33% increase in endogenous dopamine plus noise (circles). Fit to the noisy data (dashed line). See text for details.

Human study

Analysis of measurements analyzed with the LSSRM and $\tau = 0$ showed clear evidence for displacement of raclopride by the motor planning task. Bilateral activation was detected in the putamen and the caudate nucleus. Fig. 3 shows the TAC extracted from an activated region and the fit obtained after varying τ. Immediately following the ini-

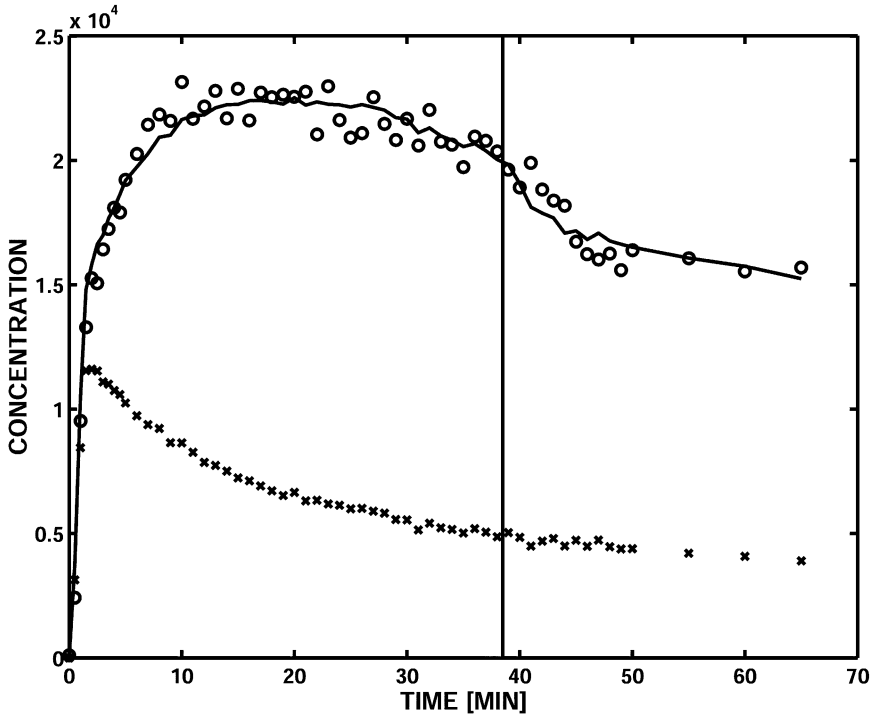

Fig. 3. Time activity curve (TAC) and fit to data from a human study. The circles symbols indicate the positron emission tomographic (PET) concentration in an "activated" putamen voxel. The vertical line at $t = 38$ min denotes the start time of the activation task. The $\times$ symbols indicate PET concentrations from the reference region TAC. The solid line is the linear simplified reference region model (LSSRM) fit with $\tau = 0.221$/min.

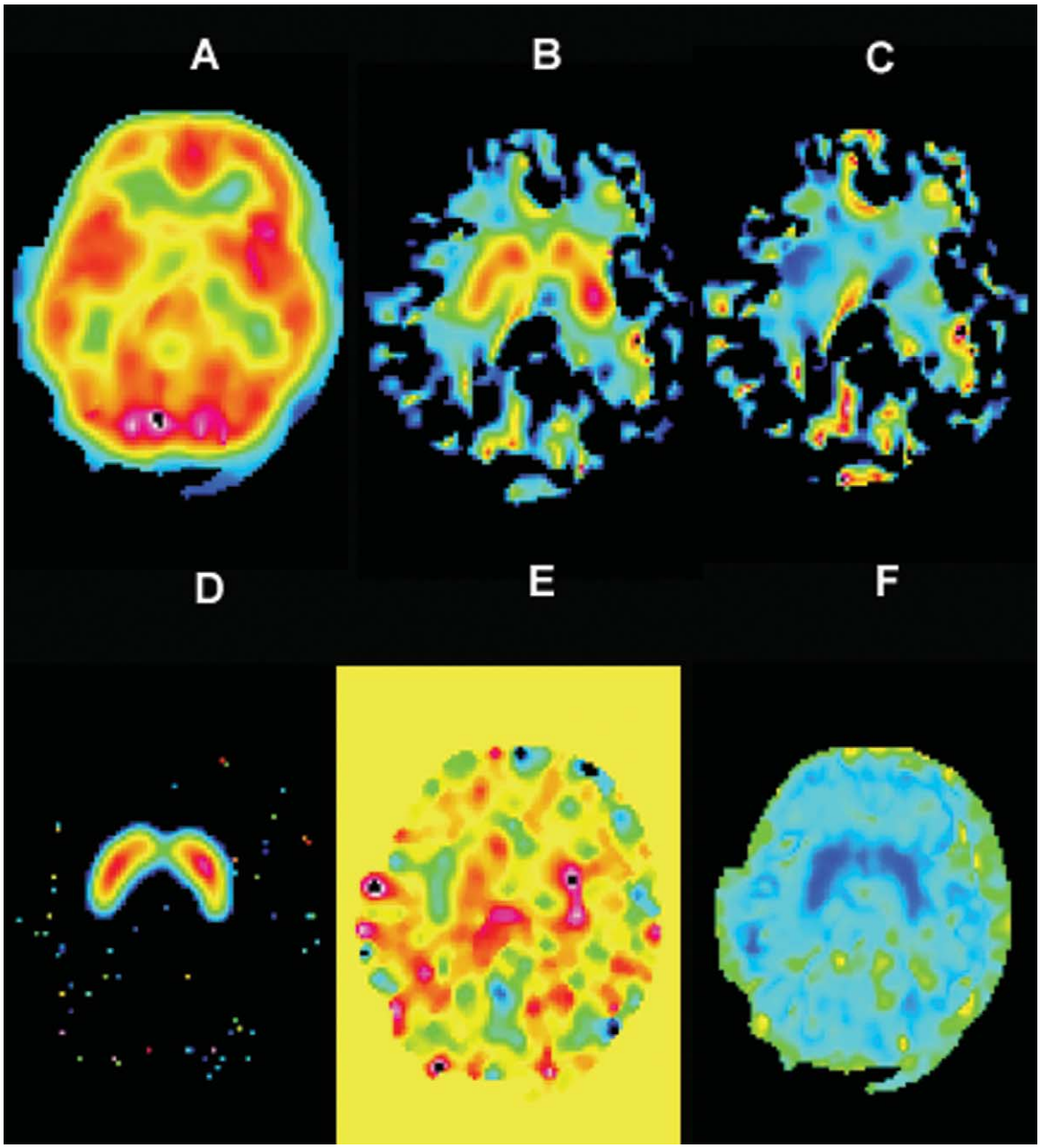

Fig. 4. Parametric images in transverse section. (A) Image of R. (B) Image of k_2. (C) Image of k_{2a}. (D) Image of binding potential. (E) Image of γ. (F) Image of SE(γ).

tiation of the task, a change in the putamen TAC (circle symbols) suggestive of ligand displacement can be observed; whereas, no changes is seen in the reference TAC. The LSSRM parameter estimates were $R = 1.154 \pm 0.0451$, $k_2 = 0.242 \pm 0.010$, $k_{2a} = 0.0653 \pm 0.0035$, and $\gamma = 0.0283 \pm 0.0054$. This leads to an estimate of $BP = 2.704$ and an observed t score of 5.3, with $df = 56$, rejects the null hypothesis $\gamma \leq 0$. The parametric maps were recomputed with $\tau = 0.22$ min^{-1}.

Fig. 4 presents an example of the parametric imaging results. There are six panels, all from the same slice. The basic parameters of the SRRM are illustrated in the top row. The binding potential (panel D) is computed from panel B and C as $k_2/k_{2a} - 1$. Panel E shows the image of γ; whereas, panel F shows the standard error of γ as computed voxel-by-voxel from the estimate of the covariance matrix. Panel E presents both positive (yellow $\rightarrow$ red) and negative estimates of γ (blue $\rightarrow$ yellow). Examination of panel F shows high values of the standard error in γ everywhere except in the striatum. Accordingly, computation of t scores will typically yield smaller values outside the striatum.

Fig. 5 illustrates the fusion of the t score ($t > 3$, $df = 56$) computed voxel-by-voxel as the ratio γ/SE(γ). Visual inspection shows that there is statistically significant increase in ligand displacement rate bilaterally in the putamen and right caudate nucleus.

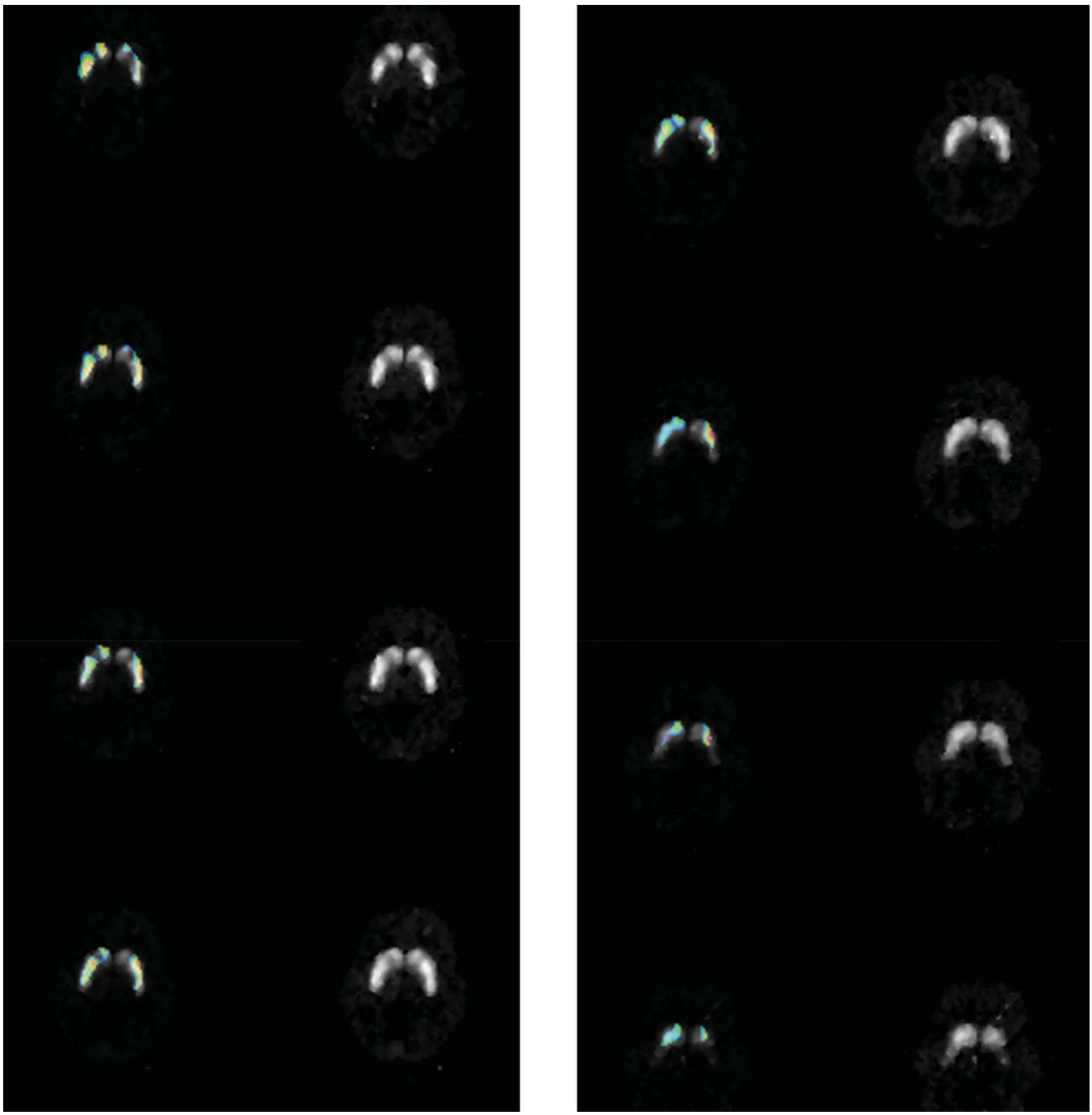

Fig. 5. Displacement of ligand by cognitive activation: The two panels show transverse sections through the putamen and caudate nucleus. The sections start near the dorsal aspect of the putamen, top of left panel, and progress in 2.4-mm steps to the basal aspect, bottom of right panel. At each level on the right is shown the parametric image of binding potential; on the left is a fusion of the t map ($t > 3$) for ligand displacement with the binding potential map.

Discussion

There are a number of ways to design and analyze a cognitive neuromodulation study. Koepp et al. (1998) measured binding potential in two separate studies, a control and an activation state. This design has the virtue of simplicity of analysis because standard techniques such as the SRRM can be used to measure binding potential in the two states. However, this design is actually more complex than it appears on the surface. The analysis depends on quantitative comparison of the binding potential, but measurement of binding potential in the activated state assumes that the subject is in steady state during activation. In fact, such measurements take 40–90 min and the effects attributed to adaptation, learning, and habituation make the steady-state assumption questionable. Furthermore, the need for two separate measurements and quantitative comparison of the binding poten-

tial introduces a source of experimental error that may reduce the sensitivity of this design.

The design employed by Pappata et al. (2002) is a clear advance since it accepts that effects may be transient and uses alternating blocked stimuli (i.e., different tasks) in a single-scan design. Their analysis follows the approach of Friston et al. (1997). The PET curve is modeled as a weighted sum of curve shapes describing the null hypothesis (i.e., no activation), shapes describing the effects of cognitive ligand displacement, and CBF-related changes. The curve shape for the null hypothesis of no activation is based on previous measurements in other subjects; whereas, curve shapes modeling cognitive ligand displacement or CBF-related changes come from simulation. Hypothesis testing is effected within the general linear statistical model by testing whether the weight of a particular curve shape is significantly greater than zero. However, the curve shapes for the control state are not specific to the subjects analyzed; and while the simulated curves are likely to be similar to the effects they model, they are not derived from real data. On this basis, one expects the model predictions to resemble the measured data but not to fit it in detail. No data were presented regarding the ability of this model to fit measured data and no data were presented regarding the covariance of the model parameters. The use of canonical curve shapes is guaranteed to inflate the sum of squared differences between the model prediction and the data, and since the error variance is directly proportional to the sum of squares, the variance of parameter estimates will increase as well. Accordingly, it is likely that the approach of Friston and colleagues (1997) is not optimal in a statistical sense.

This study proposes an analysis, the LSSRM, that is based on a kinetic model of the processes involved. The effects, or lack thereof, are estimated by fitting the model to data from individual subjects. Non-steady-state effects are included by making the parameters time dependent. The simulations reported here were informed and focused by analyzing data from human studies. We used results from a human study to set τ, the rate of decline in activation effect, in our simulations. We found that $\tau \approx 0.2$ min^{-1}, suggesting, for the task studied, that the effect is nearly abolished by 10 min after the activation is initiated. A series of simulation studies, using the standard receptor model as input, illustrate the basic properties of the method. We found using simulations of the "no activation" state with noise-free data that the LSSRM fit the data very well. There was significant bias in the parameter estimates; but the bias in the binding potential was very small. Due to the structure of the model, there is high correlation between k_2 and k_{2a}. The bias in the parameter estimates is a characteristic of the simplified reference region model and arises from the fact that the assumption of instantaneous equilibrium is not truly satisfied.

In our examination of the LSRRM, we found that model identifiability is limited to one time-dependent parameter. This finding is due to the simple shape of the PET curves. It may be possible to employ different experimental designs or task strategies to make more complex alterations in the kinetics and hence to improve identifiability. With $\tau = 0.22$ min^{-1} the duration of the perturbation is limited and the covariance structure of model parameters reduces the model identifiability, a finding that can be understood on an intuitive basis. That is, when the perturbing effects are short-lived, there are likely to be an infinite number of parameter sets that can fit the data about as well as one another. Simulations with noisy data, similar in amplitude to that observed in experiment, show that a high detection threshold will be necessary for single-subject designs to control the false positive rate because with noisy data and low thresholds one expects a higher type II error. A more conservative approach to control of type I and type II error would be to use cohorts of subjects, combining the LSSRM with the methodology described by Aston et al. (2000) or possibly with an SPM-like analysis that accounts for between-subject variability.

Dagher et al. (1997) and Pappata et al. (2002) have discussed the ambiguities that can arise from CBF-related effects. As noted in these studies, the available data are not definitive regarding how serious these effects are in practice. We know from activation studies with ^{15}O-H_2O (e.g., Hurtig et al., 1994) and fMRI that sensory-motor tasks produce large flow changes. Changes from cognitive activation tasks are usually much smaller, typically less than 15% (Andreasen et al., 1996). Jueptner et al. (1997) reported striatial activation in motor learning tasks with CBF increases in the range of 2–4%. Simulations of the activation state demonstrated that the LSSRM fits the data well even in situations where CBF-related effects were on the order of 20%. We distinguish the following three cases: (1) ligand transport rate increases with constant distribution volume, (2) plasma to tissue transport (K_1) increases more than clearance rate, and (3) clearance rate increases more than transport. In the first case, our simulations as well as those of Dahger et al. (1997) and Pappata et al. (2002) show that the changes in the PET binding curve are negligible. In the second case, transient increase in the PET binding curve was demonstrated by simulation. When analyzed with the LSRRM (fixing $\alpha = 0$ and $\beta = 0$ and letting γ vary), we were able to fit the data with negative values of γ. We interpret that to mean that increased transport, without ligand displacement, can be distinguished from the effect of interest. In the third case, the binding curve is similar to that obtained with ligand displacement and the LSRRM is unable to distinguish CBF-related effects. We do not know if, or to what degree, case 3 exists in practice; however, it does not seem likely that CBF-related changes will be a serious problem in ligand displacement studies using cognitive activation.

The results of our simulations should be evaluated in the light of the assumptions we made. First, we assumed that changes in model parameters occurred immediately after activation was initiated. Second, we not only assumed that the activation effect diminished with time but also that the decrease in effect was exponential. Therefore, these simu-

lations could be taken as a point of departure for experimental designs that might seek to increase sensitivity by prolonging the effects or otherwise blunting habituation or overlearning of a cognitive or behavioral task.

A number of observations can be made about the LSSRM approach. First, LSSRM offers a simple computational scheme. The data indicate it can make high quality parametric maps of the parameters of the SRRM of Gunn et al. (1997). Second, we found strong evidence of ligand displacement. Using an ROI targeted to a single voxel in the activated region we extracted a TAC whose shape was very similar to the predictions of the simulations. Third, these data provide the first direct evidence for the short duration of neuromodulatory effects in human subjects performing a cognitive task. Finally, further research is needed to evaluate the possibility of extending the method to different dopaminergic receptors and to other neurotransmitters.

Conclusions

This study describes a novel approach to the design and analysis of experiments whose goal is to detect changes in radioligand binding elicited by cognitive/behavioral tasks or pharmacological challenge. We have presented a new theoretical approach, the LSSRM, that is model driven and facilitates computation of parametric maps. The properties of the LSSRM were studied by simulation, showing that the theory and analytic approach can accommodate the effects of CBF-related changes as well as ligand displacement. Simulations of the noise properties of the LSSRM suggested that under realistic circumstances it is possible to detect and map neuromodulation. Mapping of increased dopamine release was demonstrated in a human study.

Acknowledgments

The authors wish to thank the staff of the PET Imaging and Cyclotron Laboratories for their technical assistance. We also thank Evan Morris for valuable suggestions. R.D.B. acknowledges the support of grant T32CA09362.

References

Adam, L.E., Zaers, J., Ostertag, H., Trojan, H., Bellemann, M.E., Brix, G., 1997. Performance evaluation of the whole-body PET scanner ECAT EXACT HR+ following the IEC standard. IEEE Trans. Nucl. Sci. 44, 1172–1179.

Alpert, N., Badgaiyan, R., Fischman, A., 2002. Detection of neuromodulatory changes in specific neurotransmitter systems: experimental design and strategy. Neuroimage 16, Part 2, Abst. S53.

Alpert, N.M., Berdichevsky, D., Levin, Z., Morris, E.D., Fischman, A.J., 1996. Improved methods for image registration. Neuroimage 3, 10–18.

Andreasen, N.C., Arndt, S.C., Cizadlo, T., O'Leary, D.S., Watkins, G.L., Boles-Ponto, L.L., Hichwa, R.D., 1996. Sample size and statistical power in [^{1}5O]H_2O studies of human cognition. J. Cereb. Blood Flow Metab. 16, 804–816.

Aston, J.A., Gunn, R.N., Worsley, K.J., Ma, Y., Evans, A.C., Dagher, A., 2000. A statistical method for the analysis of positron emission tomography neuroreceptor ligand data. Neuroimage 12, 245–256.

Badgaiyan, R.D., Fischman, A.J., Alpert, N.M., 2003. Striatal dopamine release during unrewarded motor task in human volunteers. NeuroReport 14(8), in press.

Coull, J.T., 1998. Neural correlates of attention and arousal: insights from electrophysiology, functional neuroimaging and psychopharmacology. Prog. Neurobiol. 55, 343–361.

Dagher, A., Gunn, R.N., Lockwood, G., Cunningham, V.J., Grasby, P.M., Brooks, D.J., 1998. Measuring neurotransmitter release with Positron Emission Tomography: methodological issues, in: Carson, R., Daube-Witherspoon, M., Herscovitch, P. (Eds.), Quantitative Functional Brain Imaging with Positron Emission Tomography. Academic Press, San Diego, pp. 449–454.

Endres, C.J., Carson, R.E., 1998. Assessment of dynamic neurotransmitter changes with bolus or infusion delivery of neuroreceptor ligands. J. Cereb. Blood Flow Metab. 18, 1196–210.

Farde, L., Eriksson, L., Blomquist, G., Halldin, C., 1989. Kinetic analysis of central [^{11}C]Raclopride binding D_2dopamine receptors studied by PET—a comparison to the equilibrium analysis. J. Cereb. Blood Flow Metab. 9, 696–708.

Fisher, R.E., Morris, E.D., Alpert, N.M., Fischman, A.J., 1995. In vivo imaging of neuromodulatory synaptic transmission using PET: a review of relevant neurophysiology. Hum. Brain Mapp. 3, 24–34.

Friston, K.J., Holmes, A.P., Worsley, K.J., Poline, J.B., Frith, C.D., Frackowiak, R.S.J., 1995. Statistical parametric maps in functional imaging: a general approach. Hum. Brain Mapp. 2, 189–210.

Friston, K.J., Malizia, A.L., Wilson, S., Cunningham, V.J., Jones, T., Nutt, D.J., 1997. Analysis of dynamic radioligand displacement or "activation" studies. J. Cereb. Blood Flow Metab. 17, 80–93.

Granon, S., Passetti, F., Thomas, K.L., Dalley, J.W., Everitt, B.J., Robbins, T.W., 2000. Enhanced and impaired attentional performance after infusion of D1 dopaminergic receptor agents into rat prefrontal cortex. J. Neurosci. 20, 1208–1215.

Greenwald, B.S., Davis, K.L., 1983. Experimental pharmacology of Alzheimer disease. Adv. Neurol. 38, 87–102.

Gunn, R.N., Lammertsma, A.A., Hume, S.P., Cunningham, V.J., 1997. Parametric imaging of ligand-receptor binding in PET using a simplified reference region model. Neuroimage 6, 279–287.

Hurtig, R.R., Hichwa, R.D., O'leary, D.S., Boles-Ponto, L.L., Narayana, S., Watkins, L., Andreasen, N.C., 1994. The effects of timing and duration of cognitive activation in 15O water PET studies. J. Cereb. Blood Flow Metab. 14, 423–440.

Jaber, M., Robinson, S.W., Missale, C., Caron, M.G., 1996. Dopamine receptors and brain function. Neuropharmacology 35, 1503–1519.

Jackson, S.R., Marrocco, R., Posner, M.I., 1994. Networks of anatomical areas controlling visuospatial attention: Models of neurodynamics and behavior. Neural Networks 7, 925–944.

Jentsch, J.D., Roth, R.H., Taylor, J.R., 2000. Role for dopamine in the behavioral functions of the prefrontal corticostriatal system: implications for mental disorders and psychotropic drug action. Prog. Brain Res. 126, 433–453.

Jueptner, M., Frith, C.D., Brooks, D.J., Frackowiak, R.S., Passingham, R.E., 1997. Anatomy of motor learning. II. Subcortical structures and learning by trial and error. J. Neurophysiol. 77, 1325–1337.

Kahkonen, S., Ahveninen, J., Jaaskelainen, I.P., Kaakkola, S., Naatanen, R., Huttunen, J., Pekkonen, E., 2001. Effects of haloperidol on selective attention: a combined whole-head MEG and high-resolution EEG study. Neuropsychopharmacology 25, 498–504.

Kimberg, D.Y., Aguirre, G.K., Lease, J., D'Esposito, M., 2001. Cortical effects of bromocriptine, a D-2 dopamine receptor agonist, in human subjects, revealed by fMRI. Hum. Brain Mapp. 12, 246–257.

Koepp, M.J., Gunn, R.N., Lawrence, A.D., Cunningham, V.J., Dagher, A., Jones, T., Brooks, D.J., Bench, C.J., Grasby, P.M., 1998. Evidence for striatal dopamine release during a video game. Nature 393, 266–268.

Kulisevsky, J., 2000. Role of dopamine in learning and memory: implications for the treatment of cognitive dysfunction in patients with Parkinson's disease. Drugs Aging 16, 365–379.

Lammertsma, A.A., Bench, C.J., Hume, S.P., Osman, S., Gunn, K., Brooks, D.J., Frackowiak, R.S., 1996. Comparison of methods for analysis of clinical [11C]raclopride studies. J. Cereb. Blood Flow Metab. 16, 42–52.

Lammertsma, A.A., Hume, S.P., 1996. Simplified reference tissue model for PET receptor studies. Neuroimage 4, 153–158.

Lawrence, A.D., Weeks, R.A., Brooks, D.J., Andrews, T.C., Watkins, L.H., Harding, A.E., Robbins, T.W., Sahakian, B.J., 1998. The relationship between striatal dopamine receptor binding and cognitive performance in Huntington's disease. Brain 121, 1343–1355.

Morris, E.D., Fisher, R.E., Alpert, N.M., Rauch, S.L., Fischman, A.J., 1995. In vivo imaging of neuromodulation using positron emission tomography: optimal ligand characteristics and task length for detection of activation. Hum. Brain Mapp. 3, 35–55.

Oak, J.N., Oldenhof, J., Van Tol, H.H., 2000. The dopamine D(4) receptor: one decade of research. Eur.J. Pharmacol. 405, 303–327.

Pappata, S., Dehaene, S., Poline, J.B., Gregoire, M.C., Jobert, A., Delforge, J., Frouin, V., Bottlaender, M., Dolle, F., Di Giamberardino, L., Syrota, A., 2002. In vivo detection of striatal dopamine release during reward: a PET study with [^{11}C]raclopride and a single dynamic scan approach. Neuroimage 16, 1015–1027.

Perry, E., Walker, M., Grace, J., Perry, R., 1999. Acetylcholine in mind: a neurotransmitter correlate of consciousness? Trends Neurosci. 22, 273–280.

Robbins, T.W., 2000. Chemical neuromodulation of frontal-executive functions in humans and other animals. Exp. Brain Res. 133, 130–138.

Robbins, T.W., McAlonan, G., Muir, J.L., Everitt, B.J., 1997. Cognitive enhancers in theory and practice: studies of the cholinergic hypothesis of cognitive deficits in Alzheimer's disease. Behav. Brain Res. 83, 15–23.

Searle, S.R., 1971. Linear Models. John Wiley & Sons, New York.

Witte, E.A., Marrocco, R.T., 1997. Alteration of brain noradrenergic activity in rhesus monkeys affects the alerting component of covert orienting. Psychopharmacology (Berl.) 132, 315–323.